Transformation of Sulfur Compounds in Hydrotreating of Supercritical Fluid Extraction Subfractions of Saudi Arabia Atmospheric Residua

ARTICLE *in* ENERGY & FUELS · JANUARY 2015

Impact Factor: 2.79 · DOI: 10.1021/ef5025438

7 AUTHORS, INCLUDING:

Linzhou Zhang

China University of Petroleum

16 PUBLICATIONS **47** CITATIONS

SEE PROFILE

Suoqi Zhao

China University of Petroleum

95 PUBLICATIONS **1,070** CITATIONS

SEE PROFILE

energy&fuels

Article

pubs.acs.org/EF

Transformation of Sulfur Compounds in the Hydrotreatment of Supercritical Fluid Extraction Subfractions of Saudi Arabia Atmospheric Residua

Mei Liu,[†,‡] Meng Wang,[†] Linzhou Zhang,[†] Zhiming Xu,[†] Yilong Chen,[†] Xiuying Guo,[†] and Suoqi Zhao*[,†]

[†]State Key Laboratory of Heavy Oil Processing, China University of Petroleum, Beijing 102249, China

[‡]Liaoning Shihua University, Fushun 113001, China

ABSTRACT: Atmospheric residue from Saudi Arabia (SZAR) was subjected to supercritical fluid extraction fractionation (SFEF) experiments. Four extractable subfractions (SFEF 1−4) and an unextractable end-cut were obtained. SFEF 1−4 were subjected to a hydrotreating (HDT) test in a mini-tubular reactor packed with commercial hydrodemetallization (HDM) and hydrodesulfurization (HDS) catalysts in order to determine the structural composition transformation of sulfur-containing compounds. Experiments were undertaken at a temperature of 360 °C, a hydrogen pressure of 14.7 MPa, a liquid hour space velocity (LHSV) of 0.25 h^{-1}, and a H_2/feed ratio of 650:1 (m^3/m^3). The SFEF subfractions and their products were subjected to analysis of their sulfur and nitrogen contents, using an ANTEK 7000S analyzer, and their saturates, aromatics, resins, and asphaltenes (SARA) compositions were analyzed using open column liquid chromatography. The detailed molecular composition of sulfur heteroatom species was determined by methylation, followed by positive-ion electrospray ionization Fourier transform ion cyclotron resonance mass spectrometry (ESI FT-ICR MS). In ESI FT-ICR analysis, the sulfur-containing compounds were characterized in terms of class, type (double bond equivalence, DBE), carbon number distribution, and relative abundance. According to the different number of sulfur atoms, sulfur-containing compounds can be divided into S_1 and S_2 class species. The results show that, depending on different transformation mechanisms, S_1 class species, which have less-aromatic cores, are easy to convert, no matter the side chain length. In addition, S_2 class species with less-aromatic cores and/or less carbon numbers have better hydrogenation reactivities. Meanwhile, S_2 class species with long and/or complex chains would be easy to cleavage into small ones under the reaction conditions. Compare to S_1 class species, S_2 species are more active. The potential transformation of sulfur compounds in HDT of subfractions of atmospheric residua were inferred from the DBE distribution and carbon number data by involving SFEF, methylation followed by FT-ICR MS for sulfur species of SFEF subfractions and their HDT products. The results may help understanding of the heavy oil sulfur removal sequence and catalyst/process optimization for heavy oil desulfurization and thereby assist the efficient production of clean transporation fuels.

INTRDUCTION

The petroleum refining industry has devoted tremendous effort to utilize heavy oil, because of the increasing demand for transportation fuels and the depletion of the conventional crude supply.[1] Nowadays, there are many residue-upgrading processes. Among them, the residue hydrotreating (HDT) process attracts more attention, because of its high liquid product yields, good product quality, high production flexibility, and good environmental protection.[2] However, because it is enriched with contaminants such as sulfur, nitrogen, metal-containing compounds, and highly condensed hydrocarbon molecules, such as asphaltenes, which exhibit high coking propensity, catalytic processing of atmospheric residue (AR), including hydrodemetallization (HDM), hydrodesulfurization (HDS), and hydrodenitrogenation (HDN), is still a challenging technological development.[3]

In order to improve the processing of residue, it is important to have a better understanding of heteroatom species composition. However, because of the enormous inherent complexity (appropriate feeds procurement, characterization, reactor testing, and product analysis), preliminary separation treatment on residue can help get a better result. There are many different heavy petroleum separation methods based on different properties, which include the following: solubility,[4−8] polarity,[9−11] acidity,[12,13] and molecular weight and size.[14] Zhao et al.[7] developed the supercritical fluid extraction and fractionation (SFEF) method and instruments to measure it. The dissolving capacity of the supercritical fluid will change under different extraction conditions; therefore, the heavy oil is fractionated based on their molecular weight and polarity, which facilitates the compositional or reaction behavior study on heavy petroleum and its subfractions.[7,15]

In recent years, Fourier transform ion cyclotron resonance mass spectrometry (FT-ICR MS) with inherent high resolution and mass accuracy has been recognized as a powerful technique for molecular characterization of petroleum and its distillates. A variety of work have been carried out on different heteroatom species, which include sulfur-containing compounds,[16−24] nitrogen-containing compounds,[11,25−30] and oxygenate-containing compounds.[31−38] Sulfur removal from heavy oils is an important step in producing clean ultralow sulfur fuels. However, it is difficult to elucidate exact desulfurization transformation solely based on the bulk properties.[23] The use of FT-ICR MS to characterize sulfur compounds has been reported else-

Received: November 15, 2014
Revised: January 5, 2015
Published: January 5, 2015

DOI: 10.1021/ef5025438
Energy Fuels 2015, 29, 702−710

where.[17−20] To enhance the detect ability by ESI mass analysis of the nonpolar sulfur compounds in vacuum residua, Müller et al.[17,24] converted sulfur compounds to methylsulfonium salts by reacting them with iodomethane in the presence of silver tetrafluoroborate. The methylsulfonium salts were characterized using positive-ion electrospray ionization Fourier transform ion cyclotron resonance mass spectrometry (ESI FT-ICR MS). It has been proven to be a practical way to investigate the heteroatom species of petroleum.

Yet, at the same time, there are less "real molecular" level investigations on residue and their conversion products. However, we have found that obtaining a realistic understanding of heavy oil desulfurization chemistry requires a systematic investigation of several heavy oil feeds that cover a very broad range of properties. In this study, atmospheric residue from Saudi Arabia (SZAR) was subjected to a SFEF experiment and four extractable subfractions (SFEF 1−4) and an unextractable were obtained. SFEF 1−4 were hydrotreated over two commercial catalysts in mini tubular reactor under an industrially relevant range of process conditions. Methylation followed by positive-ion electrospray ionization (ESI) and FT-ICR MS analyses were performed on the four extractable subfractions and their HDT products. The sulfur-containing compounds were characterized in terms of class, type (double bond equivalence, DBE), and relative abundance. Bulk property analysis was also performed to gain full insight of these materials. The objective was to reveal the transformation of sulfur-containing compounds in theHDT process.[39,40]

EXPERIMENTAL SECTION

Materials. The bulk properties of SZAR are shown in Table 1. The sulfur and nitrogen content of the oil samples was determined using an ANTEK 7000S analyzer (Antek, Inc., USA), in accordance with ASTM D 5453 and ASTM D 5762 methods, respectively. The saturates/aromatics/resins/asphaltenes (SARA) composition of oil samples were determined according to the Chinese Standard Analytical Method for Petroleum and Natural Gas Industry (No. SH/T0509-2010). Dichloromethane (DCM), methyl iodide (MeI), silver tetrafluoroborate, toluene, and methanol were analytical pure. The sulfur distribution of the oil samples were determined using a simulated distillation apparatus (Angilent 7890) and an chemiluminescent detector (7090).

Table 1. Properties of Atmospheric Residue from Saudi Arabia (SZAR)

property	value
ρ^{20} (g cm^{-3})	0.9682
υ^{100} (mm^2 s^{-1})	48.36
CCR (wt %)	10.99
elemental composition (wt %)	
C	84.91
H	11.15
S	3.44
N	0.29
metal content (μg g^{-1})	
Ni	22.38
V	69.95
SARA Fraction, c (wt %)	
saturates	45.88
aromatics	34.96
resins	17.36
asphaltenes	1.80

Supercritical Fluid Extraction Fractionation Experiment. SZAR was subjected to the SFEF process, which has been described elsewhere.[7,8,41] A total of four extractable subfractions and an unextractable end-cut of SZAR sample (0.7 kg) were prepared using the SFEF methodology. Normal pentane was used as the supercritical solvent and operated in programming pressure with an increasing gradient of 1.0 MPa/h. Table 2 shows the yields of SFEF fractions as a function of the SFEF extraction pressure. The extractable SFEF subfractions summed to 83.35 wt % of SZAR, and the total mass balance of the experiment reached 99.0 wt %. Approximately 1.0 wt % of feedstock remained in the extraction autoclave and pipeline, because of the high viscosity of feedstock.

Table 2. Extracted Pressure and Yield of Each Cut in SFEF Equipment

cut number	extract pressure (MPa)	yield (wt %)	comment
SFEF 1	5.30	21.16	flowable
SFEF 2	5.85	20.95	flowable
SFEF 3	6.65	21.01	unflowable
SFEF 4	10.00	21.23	unflowable
end-cut	N/A	15.65	solids

HDT Processes. SFEF 1−4 were subjected to HDT tests in a 30-mL mini tubular reactor packed with two commercial HDM and HDS catalysts: HDM-11 and HDS-33. Table 3 represents the results from the measurements of the catalysts. The SFEF subfractions HDT process is depicted schematically in Figure 1. These catalysts have been extensively used in heavy oil HDT units worldwide and are excellent representative catalysts for this study. Prior to the HDT run, the catalysts were presulfided with 2% carbon disulfide in cyclohexane for 72 h, followed by precoking with aviation kerosene for 48 h. According to the performance of the catalysts and products requirements, experiments were conducted under the following initial conditions for this atmospheric residue (AR)

Table 3. Parameters of HDM and HDS Catalysts

parameter	HDM-11	HDS-33
shape	cylindrical	cylindrical
pore volume	0.55 cm^3 g^{-1}	0.42 cm^3 g^{-1}
specific surface area	145 m^2 g^{-1}	160 m^2 g^{-1}
particle diameter	1.1−1.4 mm	1.0−1.4 mm
average pore diameter	16.7 nm	13.8 nm
bulk density	0.49 g cm^{-3}	0.60 g cm^{-3}
active species	Mo−Ni	Mo−Ni

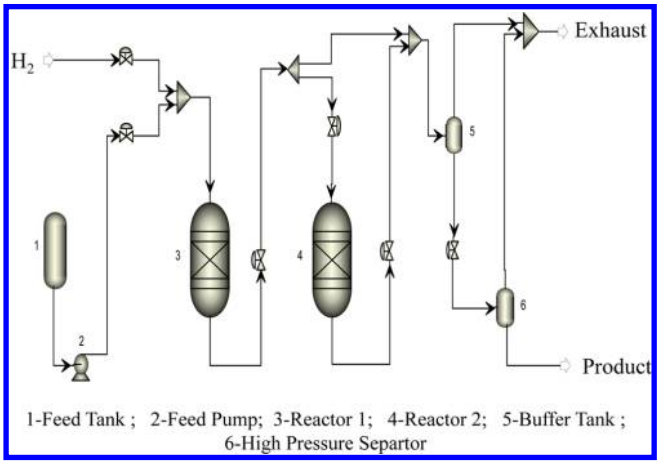

Figure 1. HDT scheme for SFEF subfractions. Reactors 1 and 2 were loaded with HDM and HDS catalysts, respectively.

DOI: 10.1021/ef5025438
Energy Fuels 2015, 29, 702−710

Table 4. Properties of SZAR, Wide Subfractions, and Their HDT Products

	SFEF 1			SFEF 2			SFEF 3			SFEF 4		
property	feed	product	conversion (%)	feed	product	conversion (%)	feed	product	conversion (%)	feed	product	conversion (%)
υ^{100} (mm^2 s^{-1})	4.432	3.694		10.27	7.82		16.9	11.94		59.51	24.73	
CCR (wt %)	0.46	0.13		1.95	0.23		2.90	0.44		10.39	3.18	
elemental analysis												
C	85.60	86.13		85.30	86.58		85.10	86.67		84.49	86.21	
H	12.27	13.15		12.01	12.84		11.76	12.66		11.34	12.36	
S	1.86	0.11	94.09	2.44	0.42	82.79	2.73	0.56	79.87	3.46	0.75	78.32
N	0.11	0.03	72.73	0.15	0.06	60.00	0.19	0.09	52.63	0.27	0.14	48.15
SARA analysis												
saturates	69.8	84.9		60.7	72.3		50.1	62.9		33.6	46.1	
aromatics	24.7	13.5		32.5	26.3		37.8	32.7		49.6	48.5	
resins	5.5	1.6		6.8	1.4		12.1	4.4		16.8	5.4	
asphaltenes	0	0		0	0		0	0		0	0	

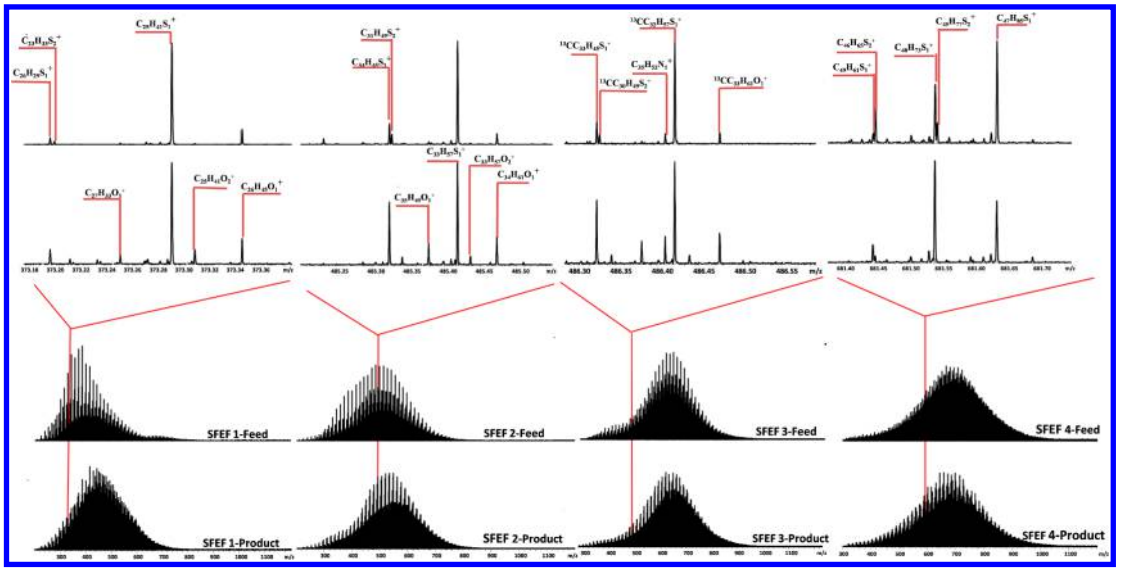

Figure 2. Broadband and expanded mass spectra for wide fractions before and after HDT, from positive-ion ESI FT-ICR MS.

in a pilot and commercial plant in China: temperature, 360 °C, hydrogen pressure, 14.7 MPa, liquid hourly space velocity (LHSV), 0.25 h^{-1}; and H_2/feed ratio, 650:1 (m^3/m^3). Analysis data reported for each data point were obtained after at least 60 h time-on-stream under a given set of conditions. Fresh catalysts was used for each feed. Depending on the number of data points collected, sometimes two fresh catalysts were used for the same heavy oil feed, to avoid any significant contribution from deactivation. Properties of SFEF subfractions and their hydrotreated products such as density, Conradson carbon residue (CCR) content, and elemental analysis, are given in Table 4. Saturates, aromatics, resins, and asphaltenes (SARA) compositional analysis was also performed.

Methyl Derivation of Sulfur Compounds. Typically, 100 mg of oil sample was resolved in 2 mL of dichloromethane (DCM). Then, 150 mg of silver tetrafluoroborate and 150 μL of methyl iodide (MeI) were added to the sample solution, in that order. The yellow precipitate (silver iodide, AgI) emerged immediately. The reaction mixture was stirred in darkness for 24 h. AgI was removed by filtration, and DCM and excess MeI in the filtrate was driven off via evaporation, using a rotary evaporator.

ESI FT-ICR MS Analysis. The samples derived form methylation were diluted with a toluene/methanol/$CHCl_3$ (1:1:1, v/v/v) mixture to a concentration of 0.02 mg/mL. The positive-ion ESI FT-ICR MS analysis was performed using a Bruker Apex-Ultra FT-ICR mass spectrometer equipped with an actively shielded 9.4 T superconducting magnet. The test samples were infused at a flow rate of 180 μL/h using a syringe pump via an Apollo II electrospray source. The conditions for positive-ion formation were as follows: emitter voltage, −4 kV; capillary column front end voltage, −4.5 kV; and capillary column end voltage, 320 V. Ions accumulated for 0.001 s in a hexapole with 2.4 V direct-current (DC) voltage and 400 Vp-p radio frequency (rf) amplitude. The optimized mass for Q1 was 200 Da. Hexapoles of the Qh interface were operated at 5 MHz and an rf amplitude of 300 Vp-p, in which ions accumulated for 0.02 s. The ICR was operated at 13 dB attenuation, a mass range of 140−1000 Da, and an acquired data size of 4 M. The time domain datasets were co-added from 128 data acquisitions.

Mass Calibration and Data Analysis. The ESI FT-ICR mass spectra were calibrated internally using a S_1 species homologous series. Peaks with a relative abundance of more than 6 times greater than the signal-to-noise ratio were exported to a spreadsheet. Elemental composition assignment for each peak was performed by custom software.[42] Species with the same heteroatom class and its isotopes with different values by double-bond equivalence (DBE) and carbon number were searched within a set of 0.0010 Kendrick mass defect (KMD) tolerance.[43,44] For each series, elemental compositions were assigned using a mass calculator program limited to molecular formulas consisting of up to 100 ^{12}C atoms, 2 ^{13}C, 200 ^{1}H, 2 ^{14}N, 5 ^{16}O, 3 ^{32}S, and 1 ^{34}S. If there is a peak series in the KMD plot of unassigned peaks, one of the peaks will be identified manually, followed by automatic searches for other species of this class.

DOI: 10.1021/ef5025438
Energy Fuels 2015, 29, 702−710

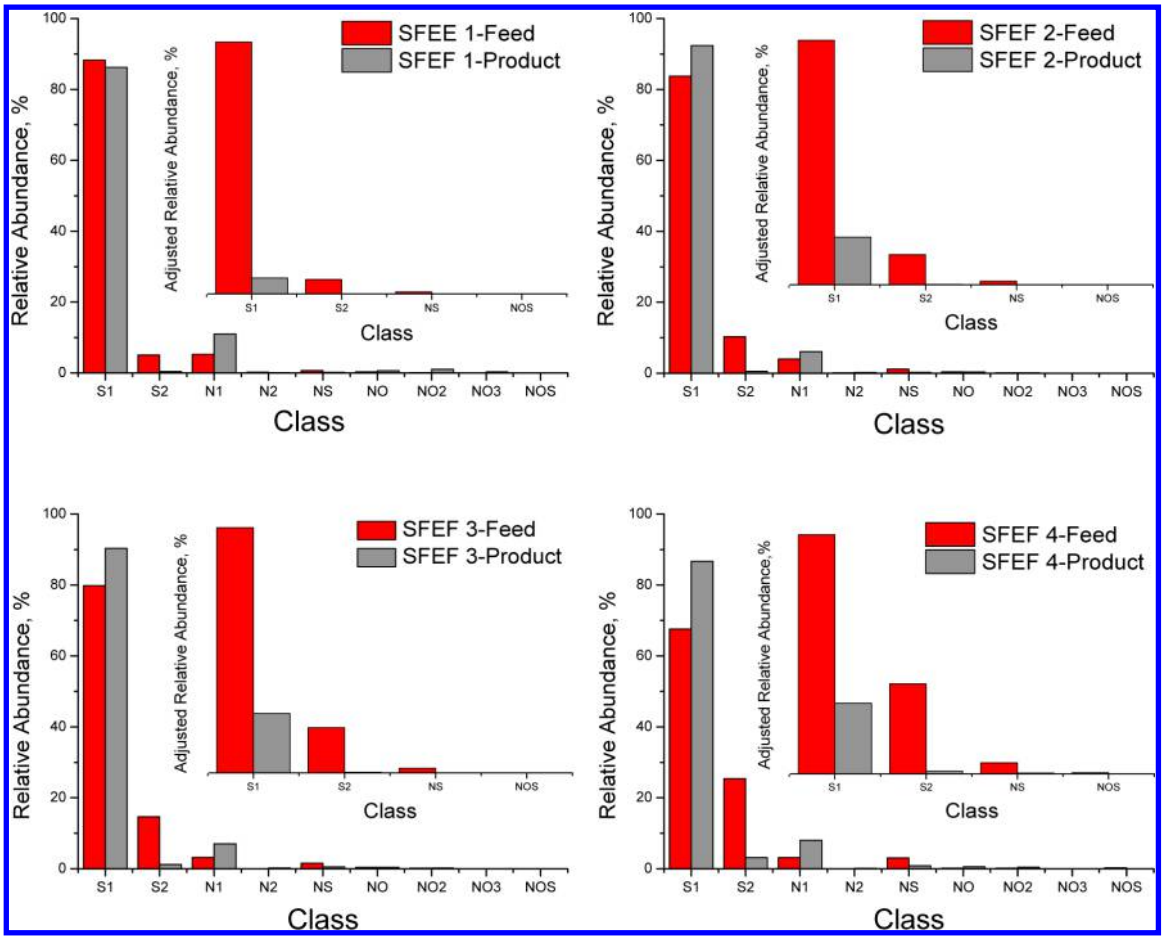

Figure 3. Relative and adjusted relative abundances of the dominant class species in SFEF fractions before and after HDT.

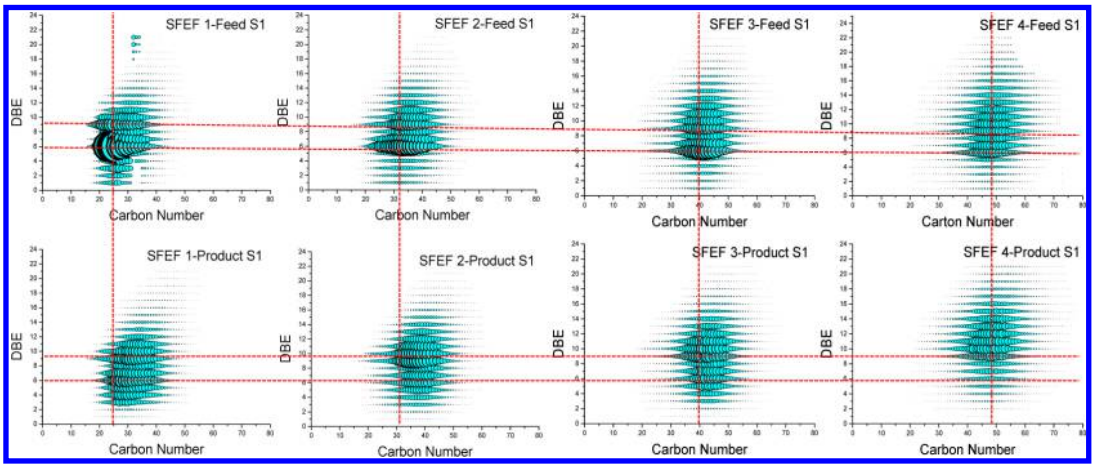

Figure 4. Dot-size plots of DBE as a function of carbon number for S_1 class species in SFEF fractions before and after HDT.

RESULTS AND DISCUSSION

The feedstock of this study, containing high-sulfur elements (3.44 wt %) and nitrogen elements (0.29 wt %) with a density of 0.9682 g/cm^3 at 20 °C. After separation via the SFEF process, the C/H ratio and total nitrogen and sulfur elemental contents of subfractions show steady growth with extracted pressure. No asphaltene was detected for all of the extracted subfractions. These indicate that the SFEF process had a good decarburization effect. After HDT, sulfur and nitrogen conversions for the four fractions were high. Sulfur-containing compounds were more reactive. In the light SFEF subfractions, because of the relatively smaller molecular weight, the depth of HDS and HDN were higher.

Figure 2 shows the broadband and expanded positive-ion ESI FT-ICR MS spectra of SFEF 1−4 before and after HDT. The mass spectrum range and maximum peak of the SFEF subfractions increased as the subfraction became heavier. The most abundant peaks of the extractable SFEF subfractions varied from m/z 400 in SFEF 1 to m/z 700 in SFEF 4. The mass range of SFEF 1 was 200−800, and that of SFEF 4 was 300−1100. Distinct disparity in composition among the SFEF subfractions

DOI: 10.1021/ef5025438
Energy Fuels 2015, 29, 702−710

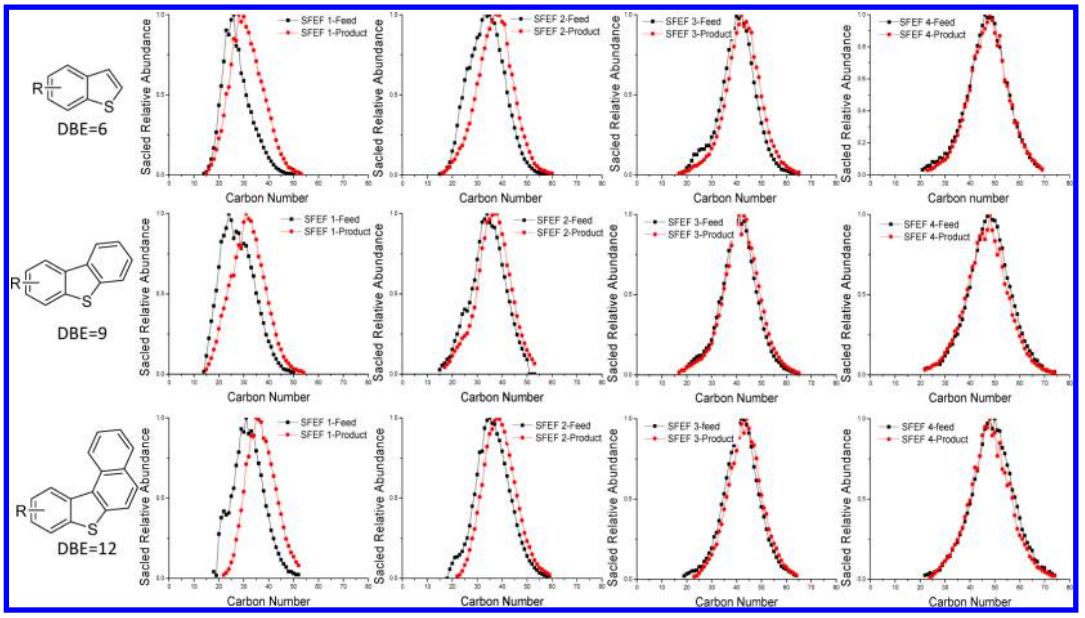

Figure 5. Transformation of DBE = 6, 9, and 12 thiophene compounds in SFEF fractions before and after HDT. For each fraction, the DBE distribution was rescaled by its highest point.

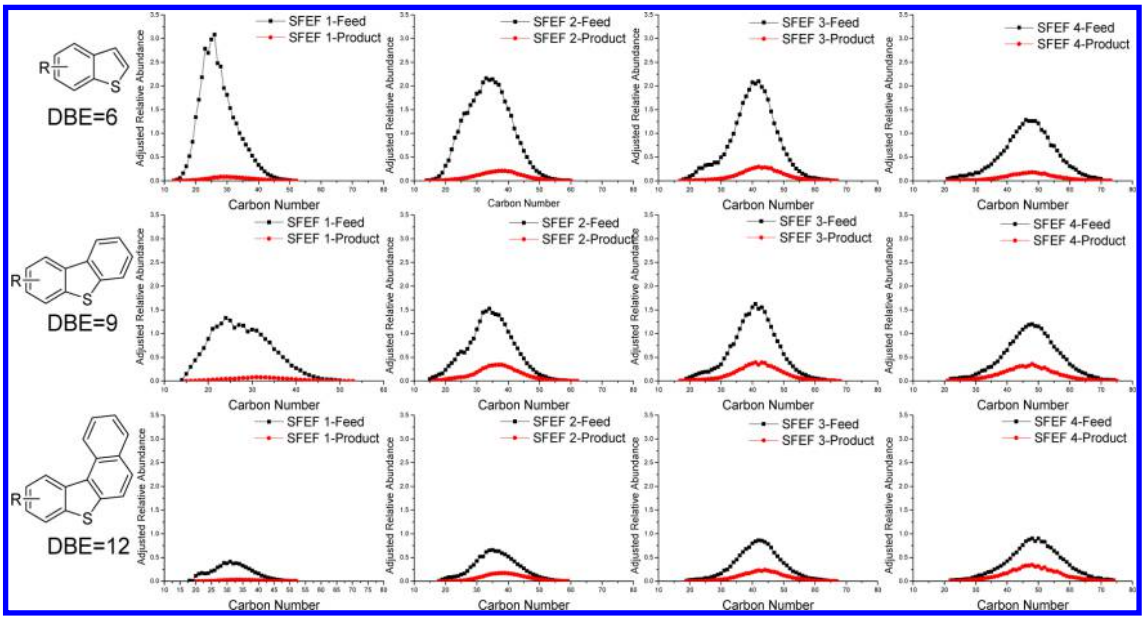

Figure 6. Adjusted relative abundance distribution of DBE = 6, 9, and 12 for S_1 class species in SFEF fractions before and after HDT.

was observed, indicating the effectiveness of SFEF heavy oil separation. After HDT, sulfur compounds with small molecular masses were readily removed, which resulted in the shift of the spectrum to a higher mass range. Meanwhile, because the SFEF 4 has high sulfur content and high molecular weight, the change was insignificant. The expanded scale mass spectra become segmented after HDT processing. The peak identifications were obtained without subtraction of the mass of the derivatization group. Compared to S_1, obviously, the relative contents of S_2 class species were decreased after HDT.

As shown in Figure 3, a total of nine class species were identified from the mass spectra: S_1, S_2, N_1, N_2, NS, NO, NO_2, NO_3, and NOS. The relative abundance of S_1 class species was 88% in SFEF 1 and decreased to 68% in SFEF 4. The relative abundance of multiheteroatom class species had undergone substantial surges as the SFEF fraction became heavier. After HDT, a prominent class changes between the S_1 and S_2 class species can be observed. The height of the peak was not relative to the absolute content, so they were adjusted, using the absolute content of sulfur compounds. The adjusted relative abundance of S_1 and S_2 class species in HDT products each decreased. Having two S atoms, S_2 class species were easier to subject to thermal decomposition or priority hydrogenation. Thus, a molecular class that contains S_2 in the feed could be converted to an S_1 or CH class. This is consistent with some of previous studies.[20] Even though S_1 class species had higher content than S_2 class species before HDT, the S_2 class species were more active.

Figure 4 shows the S_1 class composition of SFEF subfractions and their corresponding HDT products. The highest peak size was set to a fixed value, while others were scaled back. The S_1 class species, which were the most abundant species in the sample, varied over a wide range of DBE (1−33) and carbon

DOI: 10.1021/ef5025438
Energy Fuels 2015, 29, 702−710

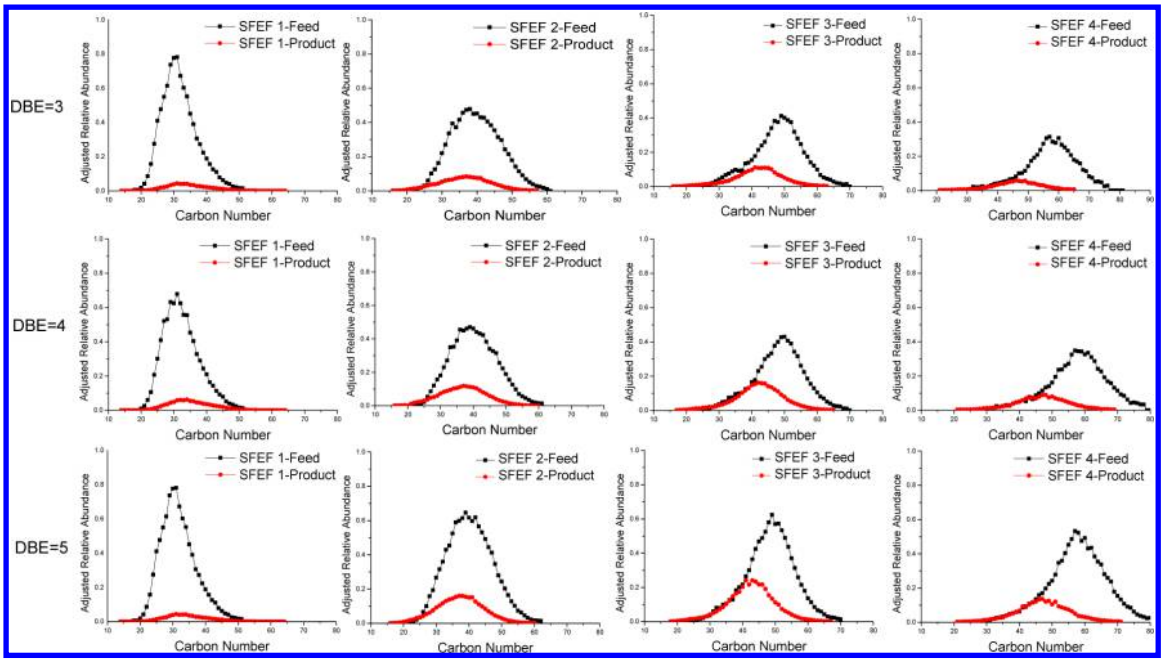

Figure 7. Adjusted relative abundance distribution of DBE = 3, 4, and 5 for S_1 class species in SFEF fractions before and after HDT.

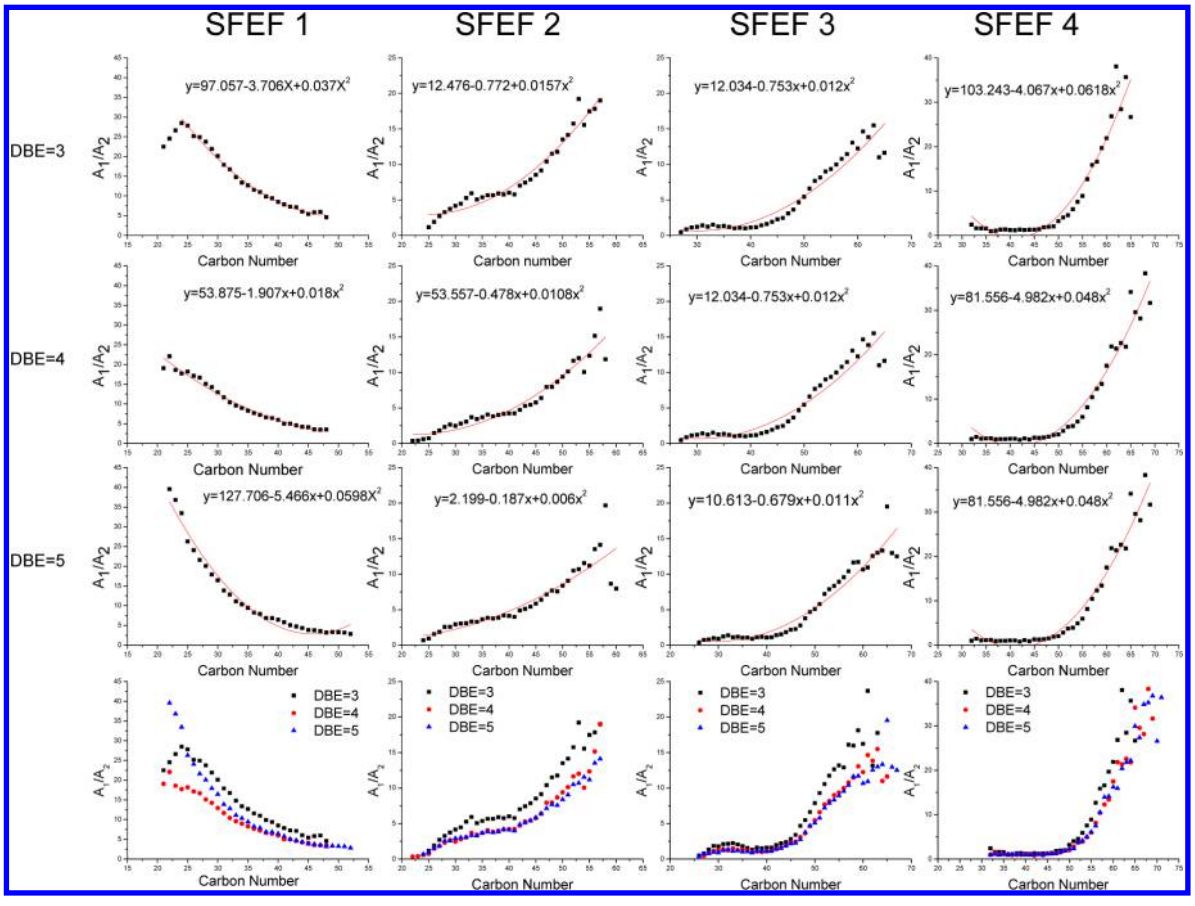

Figure 8. Curves of peak height ratio (A_1/A_2), as a function of the carbon number, for the DBE = 3, 4, 5 S_1 class species in SFEF fractions and their HDT products. A_1/A_2 was the peak height ratio before and after HDT.

number (12−75). The S_1 class species with DBE values equal to 6, 9, and 12 were dominant in SFEF 1−4 and their products. The center of the iso-abundance plots moved to the top right, molecular weights and DBE of the S_1 species were increased slightly as the SFEF subfraction became heavier. After HDT, given the SFEF subfractions, less and/or shorter alkyl side chains were readily removed, which seems to be the primary cause of the hydrogenization process. The resulting evidence shows the existence of many S_1 class species with DBE values of 1 and 2 (sulfides with one and two cyclic rings).[23] In addition, in heavier

DOI: 10.1021/ef5025438
Energy Fuels 2015, 29, 702−710

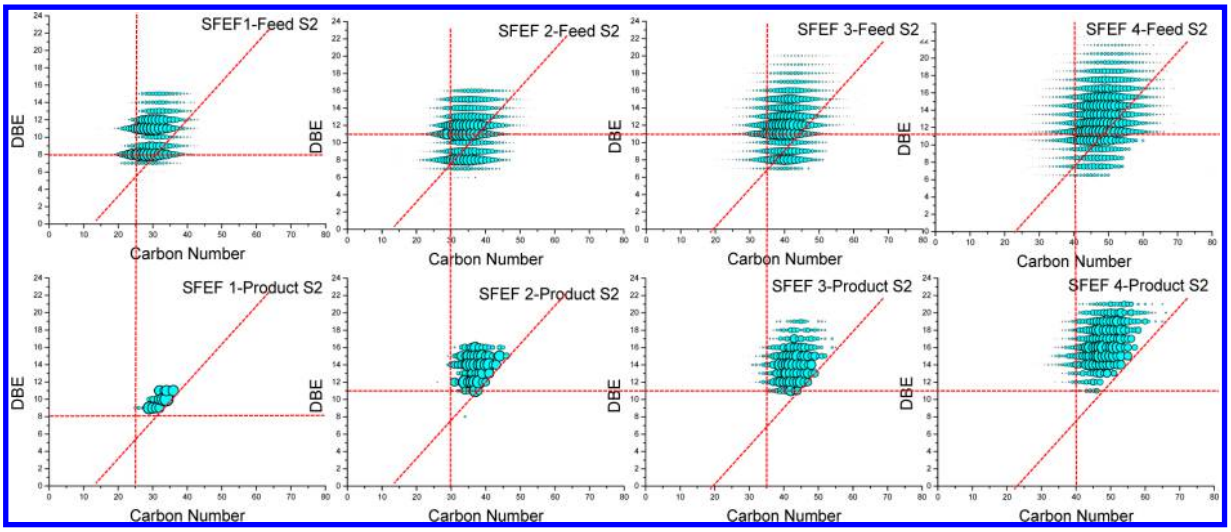

Figure 9. Dot-size plots of DBE as a function of carbon number for S_2 class species in SFEF fractions before and after HDT.

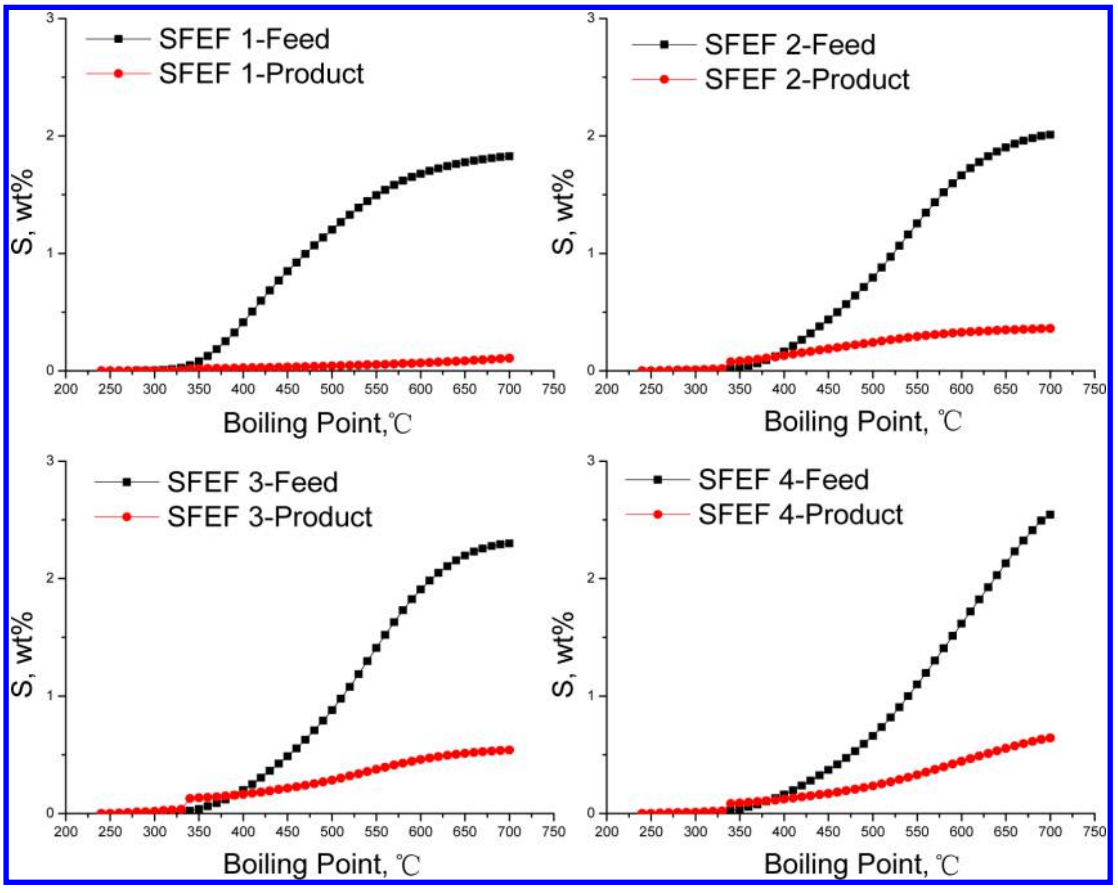

Figure 10. Sulfur distribution of SFEF fractions and their HDT product.

SFEF subfractions, larger molecular weights that have long alkyane side chains are also easy to convent. These observations support those of previous studies,[23,45] in which the loss of alkane chains results in a reduction in the molecular size. Moreover, because of less aromatic rings and the diffusional resistance, there was a dramatical decrease of benzothiophene homologues series (DBE = 6) in all the subfractions and dibenzothiophene homologues series (DBE = 9), in the light SFEF subfractions.

Figure 5 shows the relative abundance as a function of carbon number for S_1 class species with DBE = 6, 9, and 12. The most abundant S_1 compounds with DBE = 6 in SFEF 1, 2, 3, and 4 had carbon numbers of 25, 35, 40 and 47, respectively. After HDT, distribution with the maxima increased to 31, 36, 42, and 48. Figure 5 indicates that benzothiophene with fewer alkyl side chains were more readily removed by HDT. It illustrates the effect of alkyl side chains on the adsorption of sulfur-containing molecules on the catalyst surface. Meanwhile, benzothiophene homologues with long or multisubstituted side chains decreased steadily, because of side-chain bond breaking. Similar trends were observed for compounds with DBE = 9 and DBE = 12. Figure 6

DOI: 10.1021/ef5025438
Energy Fuels 2015, 29, 702−710

showed the adjusted relative abundance of benzothiophene, dibenzothiophene, and benzonaphthothiophene homologues in the SFEF subfractions and their HDT products. It is clear that the contents of benzothiophene homologues were decreased slightly as the SFEF subfraction became heavier. In contrast, the contents of benzonaphthothiophene homologues were increased. After HDT, the contents of three types of compounds, especially benzothiophene homologues, were obviously reduced. In the light subfractions, the peak shifted to the right, illustrating the effect of alkyl side chains on the adsorption of sulfur-containing molecules on the catalyst surface. This consistent with the work of Zhang et al., who described the phenomenon of nitrogen-containing compounds.[30] In the heavy subfractions, because of the influence of cleavage into small ones, the peak shifted to the left. These were completely consistent with the trends shown in Figure 3.

Figure 7 showed the adjusted relative abundance of DBE = 3, 4, 5 for the S_1 class species in the SFEF subfractions and their HDT products. For the DBE = 3, 4, and 5 sulfur-containing compounds, as the SFEF subfraction became heavier, the adjusted relative abundance was decreased. After HDT, except for SFEF 1, the peak shifted to the left. Given the comprehensive previous research results regarding benzothiophene, dibenzothiophene, and benzonaphthothiophene homologues (Figure 6), it is obvious that the molecules with smaller DBE values and long alkane chains tend to cleave into small ones and then undergo desulfurization. As the value of DBE increased, side-chain cleavage became difficult; the effect of aromatic bond hydrogenation is more apparent.

The abscissa is carbon number and the ordinate is the peak height ratio before and after HDT process (see Figure 8). It is clear that the change trends of the same wide subfraction of three types of sulfur-containing compounds were basically identical. A dualistic simple equation is obtained by fitting the test date. In the lighter subfraction (SFEF 1), lower molecular sulfur-containing compounds changed obviously. In contrast, in the heavier subfractions (SFEF 2−4), the change of larger molecular sulfur-containing compounds were more obvious.

Figure 9 shows the iso-abundance plots of S_2 class species in SFEF subfractions before and after HDT. Their trends in DBE and carbon number variations those classes are similar to their S_1 class analogues. It is clear that, as the SFEF subfraction became heavier, the DBE distribution of SFEF subfractions and products shifted to the right. After HDT, S_2 class species with low molecular weights and/or low DBE values that can achieve closer contact to the catalytic sites were readily removed. In addition, we can also get a slash, the aromaticity slope (DBE/carbon number ratio) of the reactant were 0.25 for the oblique line, under which S_2 species were easily cleaved to small ones.

Figure 10 shows the sulfur distribution of SFEF subfractions. It is clear that, as the subfractions became heavier, the sulfur content increased as the temperature increased. After HDT, the sulfur contents of the four wide subfractions were significantly lower; among them, the change of the lighter subfractions were more obvious. Interestingly, there was a sudden increase at ∼330 °C. This phenomenon is further evidence that the macromolecular side-chain cleavage make the sulfur contents within the scope of the low boiling point higher after the HDT process.

CONCLUSION

FT-ICR-MS analyses were performed on SFEF subfractions of atmospheric residue (AR) from Saudi Arabia before and after HDT. The AR was successfully separated into four wide fractions, each with a yield of 20 wt %, from light to heavy properties and compositions. The HDT results showed that the lighter SFEF cuts get a higher sulfur removal rate under same HDT conditions. The relative abundance of the multifunctional group class of SFEF 1−4 and their HDT products, such as S_1, S_2, and N_1, is growing gradually with the SFEF pressures. Compared to the S_1 class species, S_2 species are more active. S_1 class species have less-aromatic cores, which are easy to convert, no matter the side-chain length. In addition, S_2 class species with less-aromatic cores and/or less carbon numbers have better hydrogenation reactivities. More-alkyl side chains increase the probability of S_2 cleavage into smaller ones.

AUTHOR INFORMATION

Corresponding Author

*Tel.: +86-10-8973-9015. Fax: +86-10-6972-4721. E-mail: sqzhao@cup.edu.cn.

Notes

The authors declare no competing financial interest.

ACKNOWLEDGMENTS

This work was supported by the National Natural Science Foundation of China (Nos. NSFCU1162204 and 21176254). The authors thank Quan Shi for his help in the experiments.

REFERENCES

(1) Choudhary, T. V.; Parrott, S.; Johnson, B. Unraveling Heavy Oil Desulfurization Chemistry: Targeting Clean Fuels. *Environ. Sci. Technol.* **2008**, *42* (6), 1944−1947.

(2) Zhang, D. Y. *Processing Technology of Sour Crude*; Petrochemical Press of China: Beijing, China, 2003, *408*.

(3) Rana, M. S.; Sámano, V.; Ancheyta, J.; Diaz, J. A. I. A Review of Recent Advances on Process Technologies for Upgrading of Heavy Oils and Residua. *Fuel* **2007**, *86* (9), 1216−1231.

(4) Speight, J. G.; Long, R. B.; Trowbridge, T. D. Factors influencing the separation of asphaltenes from heavy petroleum feedstocks. *Fuel* **1984**, *63* (5), 616−620.

(5) Andersen, S. I.; Speight, J. G. Thermodynamic models for asphaltene solubility and precipitation. *J. Pet. Sci. Eng.* **1999**, *22* (1−3), 53−56.

(6) Alboudwarej, H.; Beck, J.; Svrcek, W. Y.; Yarranton, H. W.; Akbarzadeh, K. Sensitivity of Asphaltene Properties to Separation Techniques. *Energy Fuels* **2002**, *16* (2), 462−469.

(7) Zhao, S.; Xu, Z.; Hu; Y. Supercritical fluid extraction fractionation—The depth of the oil and heavy oil precision separation technology. *Pet. Instrum.* **2001**, *15* (4), 12−15, 32.

(8) Xu, C.; E, H.; Chung, K. H. Predicting Vaporization of Residua by UNIFAC Model and Its Implications to RFCC Operations. *Energy Fuels* **2003**, *17* (3), 631−636.

(9) Corbett, L. W. Composition of asphalt based on generic fractionation. *Anal. Chem.* **1969**, *41* (4), 576−579.

(10) Zhou, X.; Chen, S.; Chang, K. Research of heat transfer performance for Residue oil groups. *J. East China Univ. Sci. Technol.* **1995**, *21* (6), 654−659.

(11) Zhu, X.; Shi, Q.; Zhang, Y.; Pan, N.; Xu, C.; Chung, K. H.; Zhao, S. Characterization of Nitrogen Compounds in Coker Heavy Gas Oil and Its Subfractions by Liquid Chromatographic Separation Followed by Fourier Transform Ion Cyclotron Resonance Mass Spectrometry. *Energy Fuels* **2010**, *25* (1), 281−287.

(12) Boduszynski, M. M. Composition of heavy petroleums. 2. Molecular characterization. *Energy Fuels* **1988**, *2* (5), 597−613.

(13) Ramljak, Z.; Solc, A.; Arpino, P. Separation of acids from asphalts. *Anal. Chem.* **1977**, *49* (8), 1222−1225.

(14) Coleman, H. J.; Hirsch, D. E.; Dooley, J. E. Separation of Crude Oil Fractions by Gel Permeation Chromatography. *Anal. Chem.* **1969**, *41* (6), 800−804.

DOI: 10.1021/ef5025438
Energy Fuels 2015, 29, 702−710

(15) Sun, Y.; Yang, C.; Shan, H.; Shen, B. Characterization of the Reaction Performance for Residue Hydrotreating Feedstocks. *Energy Fuels* **2010**, *25* (1), 269−272.
(16) Liu, P.; Shi, Q.; Pan, N.; Zhang, Y.; Chung, K. H.; Zhao, S.; Xu, C. Distribution of Sulfides and Thiophenic Compounds in VGO Subfractions: Characterized by Positive-Ion Electrospray Fourier Transform Ion Cyclotron Resonance Mass Spectrometry. *Energy Fuels* **2011**, *25* (7), 3014−3020.
(17) Shi, Q.; Pan, N.; Liu, P.; Chung, K. H.; Zhao, S.; Zhang, Y.; Xu, C. Characterization of Sulfur Compounds in Oilsands Bitumen by Methylation Followed by Positive-Ion Electrospray Ionization and Fourier Transform Ion Cyclotron Resonance Mass Spectrometry. *Energy Fuels* **2010**, *24* (5), 3014−3019.
(18) Liu, P.; Xu, C.; Shi, Q.; Pan, N.; Zhang, Y.; Zhao, S.; Chung, K. H. Characterization of Sulfide Compounds in Petroleum: Selective Oxidation Followed by Positive-Ion Electrospray Fourier Transform Ion Cyclotron Resonance Mass Spectrometry. *Anal. Chem.* **2010**, *82* (15), 6601−6606.
(19) Liu, P.; Shi, Q.; Chung, K. H.; Zhang, Y.; Pan, N.; Zhao, S.; Xu, C. Molecular Characterization of Sulfur Compounds in Venezuela Crude Oil and Its SARA Fractions by Electrospray Ionization Fourier Transform Ion Cyclotron Resonance Mass Spectrometry. *Energy Fuels* **2010**, *24* (9), 5089−5096.
(20) Payzant, J. D.; Mojelsky, T. W.; Strausz, O. P. Improved methods for the selective isolation of the sulfide and thiophenic classes of compounds from petroleum. *Energy Fuels* **1989**, *3* (4), 449−454.
(21) Panda, S. K.; Schrader, W.; Andersson, J. T. Fourier transform ion cyclotron resonance mass spectrometry in the speciation of high molecular weight sulfur heterocycles in vacuum gas oils of different boiling ranges. *Anal. Bioanal. Chem.* **2008**, *392* (5), 839−848.
(22) Purcell, J. M.; Juyal, P.; Kim, D.; Rodgers, R. P.; Hendrickson, C. L.; Marshall, A. G. Sulfur Speciation in Petroleum: Atmospheric Pressure Photoionization or Chemical Derivatization and Electrospray Ionization Fourier Transform Ion Cyclotron Resonance Mass Spectrometry. *Energy Fuels* **2007**, *21* (5), 2869−2874.
(23) Purcell, J. M.; Merdrignac, I.; Rodgers, R. P.; Marshall, A. G.; Gauthier, T.; Guibard, I. Stepwise Structural Characterization of Asphaltenes during Deep Hydroconversion Processes Determined by Atmospheric Pressure Photoionization (APPI) Fourier Transform Ion Cyclotron Resonance (FT-ICR) Mass Spectrometry. *Energy Fuels* **2009**, *24* (4), 2257−2265.
(24) Müller, H.; Andersson, J. T.; Schrader, W. Characterization of High-Molecular-Weight Sulfur-Containing Aromatics in Vacuum Residues Using Fourier Transform Ion Cyclotron Resonance Mass Spectrometry. *Anal. Chem.* **2005**, *77* (8), 2536−2543.
(25) von Mühlen, C.; de Oliveira, E. C.; Zini, C. A.; Caramão, E. B.; Marriott, P. J. Characterization of Nitrogen-Containing Compounds in Heavy Gas Oil Petroleum Fractions Using Comprehensive Two-Dimensional Gas Chromatography Coupled to Time-of-Flight Mass Spectrometry. *Energy Fuels* **2010**, *24* (6), 3572−3580.
(26) Shi, Q.; Zhao, S.; Xu, Z.; Chung, K. H.; Zhang, Y.; Xu, C. Distribution of Acids and Neutral Nitrogen Compounds in a Chinese Crude Oil and Its Fractions: Characterized by Negative-Ion Electrospray Ionization Fourier Transform Ion Cyclotron Resonance Mass Spectrometry. *Energy Fuels* **2010**, *24* (7), 4005−4011.
(27) Maryutina, T. A.; Soin, A. V. Novel Approach to the Elemental Analysis of Crude and Diesel Oil. *Anal. Chem.* **2009**, *81* (14), 5896−5901.
(28) McKenna, A. M.; Purcell, J. M.; Rodgers, R. P.; Marshall, A. G. Identification of Vanadyl Porphyrins in a Heavy Crude Oil and Raw Asphaltene by Atmospheric Pressure Photoionization Fourier Transform Ion Cyclotron Resonance (FT-ICR) Mass Spectrometry. *Energy Fuels* **2009**, *23* (4), 2122−2128.
(29) Qian, K.; Edwards, K. E.; Mennito, A. S.; Walters, C. C.; Kushnerick, J. D. Enrichment, Resolution, and Identification of Nickel Porphyrins in Petroleum Asphaltene by Cyclograph Separation and Atmospheric Pressure Photoionization Fourier Transform Ion Cyclotron Resonance Mass Spectrometry. *Anal. Chem.* **2009**, *82* (1), 413−419.
(30) Zhang, T.; Zhang, L.; Zhou, Y.; Wei, Q.; Chung, K. H.; Zhao, S.; Xu, C.; Shi, Q. Transformation of Nitrogen Compounds in Deasphalted Oil Hydrotreating: Characterized by Electrospray Ionization Fourier Transform-Ion Cyclotron Resonance Mass Spectrometry. *Energy Fuels* **2013**, *27* (6), 2952−2959.
(31) Fafet, A.; Kergall, F.; Da Silva, M.; Behar, F. Characterization of acidic compounds in biodegraded oils. *Org. Geochem.* **2008**, *39*, 1235−1242.
(32) Barrow, M. P.; Witt, M.; Headley, J. V. Athabasca oil sands process water: Characterization by atmospheric pressure photoionization and electrospray ionization fourier transform ion cyclotron resonance mass spectrometry. *Anal. Chem.* **2010**, *82*, 3727−3735.
(33) Qian, K.; Edwards, K. E.; Dechert, G. J.; Jaffe, S. B.; Green, L. A.; Olmstead, W. N. Measurement of Total Acid Number (TAN) and TAN Boiling Point Distribution in Petroleum Products by Electrospray Ionization Mass Spectrometry. *Anal. Chem.* **2008**, *80* (3), 849−855.
(34) Smith, D. F.; Schaub, T. M.; Kim, S.; Rodgers, R. P.; Rahimi, P.; Teclemariam, A.; Marshall, A. G. Characterization of Acidic Species in Athabasca Bitumen and Bitumen Heavy Vacuum Gas Oil by Negative-Ion ESI FT−ICR MS with and without Acid−Ion Exchange Resin Prefractionation. *Energy Fuels* **2008**, *22* (4), 2372−2378.
(35) Smith, D. F.; Klein, G. C.; Yen, A. T.; Squicciarini, M. P.; Rodgers, R. P.; Marshall, A. G. Crude Oil Polar Chemical Composition Derived from FT−ICR Mass Spectrometry Accounts for Asphaltene Inhibitor Specificity. *Energy Fuels* **2008**, *22* (5), 3112−3117.
(36) Douda, J.; Alvarez, R.; Navarrete Bolaños, J. Characterization of Maya Asphaltene and Maltene by Means of Pyrolysis Application. *Energy Fuels* **2008**, *22* (4), 2619−2628.
(37) Wang, L.; He, C.; Zhang, Y.; Zhao, S.; Chung, K. H.; Xu, C.; Hsu, C. S.; Shi, Q. Characterization of Acidic Compounds in Heavy Petroleum Resid by Fractionation and Negative-Ion Electrospray Ionization Fourier Transform Ion Cyclotron Resonance Mass Spectrometry Analysis. *Energy Fuels* **2013**, *27* (8), 4555−4563.
(38) Zhang, Y.; Shi, Q.; Li, A.; Chung, K. H.; Zhao, S.; Xu, C. Partitioning of Crude Oil Acidic Compounds into Subfractions by Extrography and Identification of Isoprenoidyl Phenols and Tocopherols. *Energy Fuels* **2011**, *25* (11), 5083−5089.
(39) Snyder, L. R.; Buell, B. E.; Howard, H. E. Nitrogen and oxygen compound types in petroleum. Total analysis of a 700−850 F distillate from a California crude oil. *Anal. Chem.* **1968**, *40* (8), 1303−1317.
(40) Gray, M. R.; Ayasse, A. R.; Chan, E. W.; Veljkovic, M. Kinetics of Hydrodesulfurization of thiophenic and sulfide sulfur in Athabasca bitumen. *Energy Fuels* **1995**, *9* (3), 500−506.
(41) Zhang, L.; Xu, Z.; Shi, Q.; Sun, X.; Zhang, Na.; Zhang, Y.; Chung, K. H.; Xu, C.; Zhao, S. Molecular Characterization of Polar Heteroatom Species in Venezuela Orinoco PetroleumVacuum Residue and Its Supercritical Fluid Extraction Subfractions. *Energy Fuels* **2012**, *26* (9), 5795−5803.
(42) Shi, Q.; Pan, N.; Long, H.; Cui, D.; Guo, X.; Long, Y.; Chung, K. H.; Zhao, S.; Xu, C.; Hsu, C. S. Characterization of Middle-Temperature Gasification Coal Tar. Part 3: Molecular Composition of Acidic Compounds. *Energy Fuels* **2012**, *27* (1), 108−117.
(43) Shi, Q. D.; Dong, Z. Y.; Zhang, Y. H.; Zhao, S. Q.; Xu, C. M. Data Processing of High-Resolution Mass Spectra for Crude Oil and Its Distillations. *Chin. J. Instrum. Anal.* **2008**, *27* (1), 246−248.
(44) Hughey, C. A.; Hendrickson, C. L.; Rodgers, R. P.; Marshall, A. G.; Qian, K. Mass Defect Spectrum: A Compact Visual Analysis for Ultrahigh-Resolution Broadband Mass Spectra. *Anal. Chem.* **2001**, *73* (19), 4676−4681.
(45) Buch, L.; Groenzin, H.; Buenrostro-Gonzalez, E.; Andersen, S. I.; Lira-Galeana, C.; Mullins, O. C. Molecular size of asphaltene fractions obtained from residuum hydrotreatment. *Fuel* **2003**, *82* (9), 1075−1084.

DOI: 10.1021/ef5025438
Energy Fuels 2015, 29, 702−710